# Practical Conceptual Design of Quieter Urban VTOL Aircraft

**Christopher Silva**          **Wayne Johnson**
christopher.silva@nasa.gov    wayne.johnson@nasa.gov
NASA Ames Research Center
Moffett Field, CA, USA

## ABSTRACT

A toolchain and process for conceptual design of VTOL rotorcraft, employing low- and mid-fidelity tools is presented. The approach is capable of providing more quantitatively-credible trades between noise, size, and cost metrics than the methods commonly used for conceptual design. In addition to a general conceptual design tool, the approach employs comprehensive analysis for trim, blade motion, and airloads; these are then used by acoustic analysis software to develop source sound, propagate it, and calculate noise metrics. A key aspect of the approach is flexibility to assess varied aircraft types and different technologies and design features. Vehicles are sized using a representative Urban Air Mobility design mission. Demonstration cases are presented for a single main rotor helicopter, quadrotor, side-by-side helicopter, and lift+cruise aircraft. Noise metrics used for demonstration are the FAA/EASA certification Effective Perceived Noise Levels for takeoff, flyover, and approach. The concept aircraft in this study are shown to achieve reductions in noise relative the initial design points, with changes in mission performance and cost as a consequence. Many of the designs are predicted to be tens of EPNdB quieter in the certification metrics than existing helicopters.

## INTRODUCTION

Conceptual design often starts with a large design space of possible solutions. Priority is therefore placed on flexibility and efficiency of problem setup and computation. This has historically been performed by applying general trends and empirical methods rather than detailed analyses. The new market of Urban Air Mobility (UAM) has introduced a number of new design degrees of freedom and constraints to be considered in conceptual design. Consequently, the empirical methods traditionally employed in conceptual design may not accurately predict the characteristics and tradeoffs of UAM vehicles. Rotor noise of UAM vehicles is expected to be a key constraint that will bound the feasibility of vehicles, and existing conceptual design tools have had difficulty in predicting noise quantitatively. For battery-powered and distributed electric propulsion aircraft which are being considered for UAM, the takeoff weight growth factor is much higher than for traditional liquid fuel powered aircraft; it is critically important to know just how much weight must be added to achieve a desired noise level, without risking an expensive spiraling of vehicle weight. NASA is working to improve the breadth, accuracy, efficiency, and ease of use of VTOL conceptual design tools and processes to address this shortcoming. The result of this work will be a toolchain and set of best practices which may be applied for practical conceptual design of multi-rotor VTOL aircraft in urban missions. The NASA Revolutionary Vertical Lift Technology (RVLT) project is developing tools and documentation to enable practical conceptual design of VTOL vehicles, as described herein.

Computing rotor noise of rotorcraft requires capturing blade and wake motion, in addition to airloads on the blades. If blade-vortex-interaction (BVI) is a factor, small differences in the relative placement of blades and vortices can have a large effect on noise and dominate the noise signature. In design, this interactional sensitivity is a challenge—but also an opportunity—as there are several design variables available to the designer which will have influence on the various noise components (Ref. 1). Sufficiently accurate computation of rotor noise to make tradeoffs in conceptual design has been uncommon, but there is clear demand for evaluating this tradeoff and there have been some recent examples (Ref. 2) of this kind of conceptual design tradeoff being performed with mid- and high-fidelity tools. Low-fidelity (blade element momentum, prescribed wake) methods often used for conceptual design have proven inadequate for rotor acoustics thus far. The aforementioned blade and wake considerations are not captured with blade-element momentum theory models, and rotor-rotor interactions are even more likely for multi-rotor vehicles often considered for UAM applications, which requires that wakes be more accurately modeled. The techniques for predicting noise using higher-fidelity tools have been established and validated in previous studies (Ref. 3). Applying these lessons, recent design work by NASA has included quantitative assessment of relative noise reduction (but not absolute values) with mid-fidelity tools (Ref. 4). Recent improvements to NDARC (Ref. 5), CAMRAD II (Ref. 6, 7, 8), and AARON/ANOPP2 (Ref.

9) make it possible to perform these trades on a conceptual design timetable and have good confidence that results are quantitatively meaningful.

A demonstration of conceptual design of UAM vehicles with quantitative noise prediction is the subject of this paper. For the demonstration, 4 different types of concept aircraft are designed, representing some of the different design features seen in aircraft proposed for UAM. The aircraft used for this demonstration all have rotors which operate in edgewise flight, and do not tilt. For the demonstration, several design parameters representing noise mitigation approaches are varied to observe the sensitivities of several vehicle metrics.

## TERMINOLOGY

The terms used by various conceptual design practitioners have sometimes been a source of confusion. For use in the context of this paper, the following terms are defined:

*Attributes*: The numerical dimensions, size, and component capabilities of a concept aircraft (*e.g.* rotor radius, gross weight, installed power, design disk loading, hover tip speed).

*Capabilities*: The predicted performance of a concept aircraft on a mission or flight condition; requirements imposed on the aircraft for communication, navigation, flight control; regulatory requirements; general things which the aircraft may be able to perform.

*Concept aircraft*: A distinct definition of an aircraft, resulting from compromises and design choices, and self-consistent in that the concept aircraft's attributes and capabilities go together (often referred to as a "closed design").

*Conceptual design*: the activity of developing an insight into what aircraft will be best suited for a mission, what a particular aircraft will be capable of, or formulating a case for further investment of aircraft of ancillary systems. Conceptual design is often the first phase of a multi-step aircraft development process, which precedes preliminary design. A key distinction between conceptual design and preliminary design is that conceptual design takes place before substantial resources are committed to the definition and development of an aircraft. The team size in conceptual design is relatively small, and the aircraft development options are numerous and perhaps nebulous at the beginning of conceptual design, but focus on a much smaller set of recommendations and options by the end of conceptual design. Quantitative predictions of aircraft attributes, operational effectiveness, and cost will be developed before preliminary design begins. Alternately, conceptual design may not be targeted at the development of any distinct concept aircraft, instead used to define other necessary developments or economic opportunities and challenges.

*Baseline aircraft*: The attributes and capabilities of a concept aircraft which will be the basis of comparison for other concept aircraft.

*Excursion*: A concept aircraft which is the result of different design decisions based upon an initial concept aircraft. Excursions often play an important role in assessing sensitivities and exploring the relative importance of different capabilities.

*Type*: The overall arrangement and components of an aircraft, or perhaps the design philosophy; such as single main rotor helicopter, quiet single main rotor helicopter, coaxial compound helicopter, conventional tiltrotor, high-efficiency tiltrotor, etc. Other authors might use "category" or "class" in place of "type."

*Variant*: An aircraft which is configured at the time of delivery with aircraft components and mission equipment specific to a mission or customer, and would take a significant amount of effort and materials to convert into a different service's variant. Examples include SH-60 as a variant of UH-60, and AH-1 as a variant of UH-1.

## CONCEPTUAL DESIGN APPROACH

The RVLT project is developing tools and documentation (referred hereafter as "toolchain" for brevity) which will be provided to the VTOL conceptual design community. To scope the tool development effort, the design process needs to be defined, and some assumptions must be made about the experience level of users, the expected level of information available, and the algorithmic approach to conceptual design. There are three key assumptions which help define the tool development:

1. **A competent conceptual design team presented with documented best practices will be able to extend the tools to their own problems.** The objective is to empower design teams composed of engineers, technologists, and inventors to solve complex and flexible aircraft conceptual design problems. The present approach to ensuring tools are usable by competent users and will achieve credible results is to develop a set of best practices and example cases, covering a design-solution-relevant portion of the relevant design space. The task of providing enough simplicity of use and protection from misuse to allow a layman to competently design aircraft is outside the scope of the present work.

2. **Improved tools.** Software improvements to the constituent tools are expected to be necessary, and therefore the software must be able to be modified for the needs of the project. Commercial software is expected to be part of the toolchain; commercial software packages will be modified with the aid of the developers of the tools. The authors have identified necessary improvements to commercial

and government-developed tools in order to adequately perform conceptual design of low-noise UAM vehicles. Some of these shortcomings are known at the outset, and others become evident as the authors apply the tools, interact with users in the design community, and acquire validation data.

3. **Exploration of the design space can be performed in multiple ways for multiple purposes; the toolchain should be usable within many design constructs.** The authors have identified numerous use cases from our experience, discussions with other practitioners, textbooks, papers, and documented case studies. The toolchain being developed should be flexible enough to be used for a large number of the use cases, even at the expense of a large number of inputs being available to define an aircraft or design study. Development and implementation of design algorithms as scripts or compiled code is expected by users of the toolchain.

The tools in conceptual design are often low- to mid-fidelity, in an attempt to meet the needs of fast computational speed and broad flexibility, while maintaining a minimal setup burden and tolerance for many unknown parameters. The conceptual design process must also efficiently find optima and facilitate an understanding of the design space.

The competing desires of flexibility and ease of setup are often addressed via rich sample cases which demonstrate best practices rather than extensive program logic to rapidly setup problems correctly for the user. In conceptual design—especially when designing a novel aircraft or a novel approach to the problem—there are many occasions when the designer must be open to simple (but physics-based) extensions of models when unconventional or new requirements push the design into unexplored spaces. Sometimes it is expedient to model the *wrong* thing in problem setup in order to evaluate the *right* result with existing tools. A simple example of modeling the wrong thing is the modeling of a V-tail in earlier versions of the NDARC design software, before the feature was explicitly included: a horizontal and a vertical tail would be modeled such that the aerodynamics, flight controls, and weights matched the expected V-tail; to report the weight or some other parameter of the V-tail, the designer would need to perform their own re-bookkeeping of the NDARC outputs.

## Present practice of conceptual design informs this approach

A large number of companies and inventors are pursuing aircraft development for Urban Air Mobility missions. Some of these projects are in the conceptual design phase, and many have moved on to the preliminary design phase or later. These projects appear to have a widely varying degree of analytic sophistication and resources available at conceptual design. Many of these projects are seeking to develop aircraft which are substantially quieter than existing rotorcraft, based on the expected need to greatly reduce the objectionable noise

experienced by the public. Objectionable noise is a major barrier to UAM operations today (Ref. 10).

There are several useful textbooks on general aircraft conceptual design (examples include Refs. 11, 12, 13, 14, and 15), but these have little coverage of lower disk loading VTOL design. Ref. 16 describes both the current state-of-the-art for low disk loading VTOL design and proposes the direction in which conceptual design should be heading.

There are several conceptual design paradigms which need to be accommodated in the present toolchain; the three which are the highest priority in our development are listed below:

A. **Design a distinct concept aircraft to a set of requirements.** Requirements themselves may be subject to variation. For example, given a mission, the design team wants to know if it is possible to meet the requirements with today's or future technology; if not, what is possible?

B. **Design an aircraft incorporating a particular technology or design approach to find a compelling capability.** For example, suppose that a new type of battery has been invented, and the design team want to see what this technology can enable.

C. **Identify trends and bounds of feasibility in a design space.** For example: The goal is to draw curves for various levels of disk loading, weight fraction, cruise efficiency trades. Perhaps there is no intention to actually design any particular instance of a vehicle; the team might be designing the airspace system or fleet mix.

Expanding on item B above, it is often the case that technological invention or availability pushes design. In these cases the nature of the design problem changes from meeting a set of requirements to discovering what is possible with the technology. Moreover, questioning whether that technology-enabled capability is compelling enough to pursue long and expensive aircraft development is the outcome of conceptual design, and a specific instance of a concept aircraft need not be defined. The toolchain accommodates this design approach, where a signature technology is investigated.

Some trends in conceptual design were considered when developing the design process and toolchain described in this paper. The introduction of higher fidelity and more breadth to design is a common characteristic; there have been papers on the topic of multi-disciplinary VTOL design (chronologically: Refs. 17, 16, 18, 2, 19). For VTOL, and in particular low-to moderate-disk loading conceptual design, the available resources are more narrowly focused on specific subsystems or analysis domains.

One trend is toward formalized multidisciplinary design, analysis, and optimization (MDAO) in conceptual design.

Another, related trend is increased use of high-fidelity tools in conceptual design.

MDAO as the overarching approach for conceptual design has been the subject of extensive and systematic research for the past three decades. MDAO is becoming rather common in aircraft conceptual design, as a structured way to explore the design space and account for the high degree of coupling between disparate components of aircraft. A number of software frameworks for MDAO (Ref. 20), (Ref. 21) have been developed and are widely used. For problems with many design variables, gradient-based optimization techniques can be particularly effective. The Modular Analysis and Unified Derivatives (MAUD) approach (Ref. 22), especially with analytic gradients computed from each discipline, is well suited for local optimization of conceptual design, when an aircraft type or a few number of aircraft types have been selected for development, since the design space is more focused on a particular region and the design space topology is simply connected with many continuous (as opposed to discrete) design variables. Problems with large numbers of design variables are likely to be important use cases, and other NASA research is advancing the state-of-the-art for those use cases (examples listed at Ref. 23). For topologically complex or discrete-value dominated design spaces, other optimization techniques are appropriate. Rather than focus on tools formulated to work efficiently with an optimization approach (e.g. rewriting software to utilize adjoint algorithms for efficient and accurate gradient calculation), the present work is reducing the burden on the user associated with applying validated tools together for relevant design problems. After the tools work together efficiently and design algorithms and use cases are documented, these or other tools can be integrated within optimization frameworks.

High-fidelity in conceptual design is often tied in with MDAO. There are efforts to bring high-fidelity to conceptual design for direct design. In cases with focused design spaces, this may be appropriate (e.g. applying a single technology to a specific type of aircraft), but often this is overly limiting the conceptual design space. There are however specific scenarios when it is necessary to perform a higher-fidelity analysis before leaving conceptual design. These higher fidelity analyses often build upon the lower fidelity analyses, such as taking propulsion limits and vehicle weights from a sizing tool and coupling comprehensive analysis for vehicle trim and rotor motion with computational fluid dynamics. Some examples of when high-fidelity analyses might need to be completed before proceeding beyond conceptual design are listed below:

- Download likely to be a major factor. An example is the tiltrotor fountain effect, Ref. 24.
- Acoustics need to be accurately predicted with high certainty. In this case, coupled RANS CFD (e.g OVERFLOW) accurately predicts rotor thickness, loading, and high speed impulsive noise sources, but does not capture broadband, engine, or gearbox/motor noise. Lattice Boltzmann CFD (e.g. Ref. 25) does accurately predict tonal and broadband noise, but rotating calculations (rotors) are presently limited to incompressible speeds and performance (power) is very inaccurate. Therefore high-fidelity noise means either supplementing with mid-fidelity or running two distinct types of high-end CFD for each point; one for noise a second analysis for power.
- Rotor-rotor interference likely to be an important factor or rotor operating outside the scope of available validation data (e.g. quadrotor interference discussed in Ref. 26 and 27; side-by-side overlap in Ref. 18 and 28).
- Propulsion system operating in a new way. For example, direct coupling of motors to rotor vibratory loads in quadrotor and lift+cruise are discussed in Ref. 29, and electric propulsion system heat rejection is discussed in Ref. 30.

There are also occasions where perhaps mid-fidelity is acceptable, but a new domain needs to be considered, broadening the analysis:

- New types of flight control. For example, RPM control Refs. 31, 32.
- SensorCraft-like aircraft, where the avionics and sensor apertures need to be sized and positioned simultaneously with the rest of the aircraft (Refs. 33, 34).

Developing design solutions within a Systems Engineering framework has also been a major trend in conceptual design. This toolchain and the results of the analyses may be integrated into a Systems Engineering framework, but we are not providing specific integration interfaces. For discussion of allocation of requirements, several possible approaches are available, including a number of subjective-quantitative methods identified as Integrated Product/Process Development (Ref. 35).

## TOOLS AND WORKFLOW

The process and tools of the present activity are depicted in Figure 1 as part of an eXtensible Design Structure Matrix diagram (XDSM). The primary tools for performing physical calculations are on the diagonal of the matrix as green rectangles, interconnections are gray lines, and data entities are parallelograms. Data transfer and inter-tool design process are managed by scripts written in Python. The clouds at either end of the diagonal indicate that this toolchain can be integrated as part of a larger process. Overall inputs are in the white parallelograms at the top, and overall outputs are white parallelograms at the left. Guided design space exploration such as parameter sweeps, optimization drivers, vehicle type comparison may be implemented in the upper-left orange-colored cloud, along with other subsystem design (e.g. propulsion, flight control). On the lower-right, the green-

colored cloud indicates where vehicle and subsystem design of higher fidelity would be added in order to verify earlier conceptual design assumptions, or capture phenomena which are inadequately addressed in earlier steps of the conceptual design process (*e.g.* a set of coupled CFD download calculations for key sizing conditions).
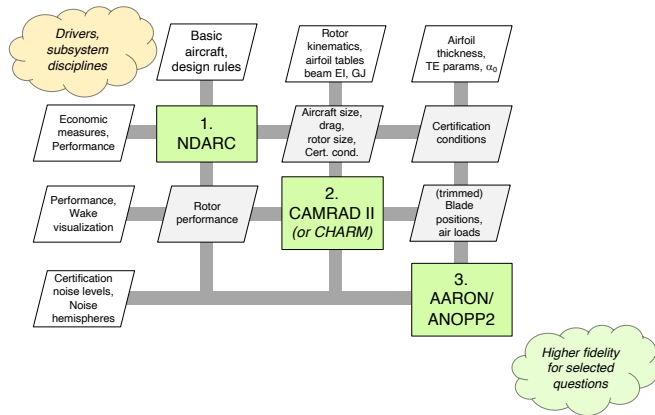


**Figure 1. XDSM diagram of the tools and workflow as the central part of a more complete conceptual design process**

For the current conceptual design demonstration, a set of parametric sweeps have been conducted with discrete values for the parameters, and no attempt to define an objective function has been performed (Figure 2).
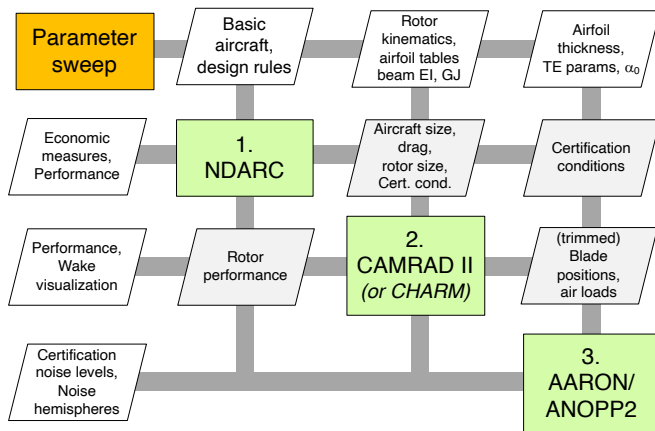


**Figure 2. XDSM diagram for the current demonstration**

## NDARC

Primary sizing and performance analysis of the aircraft is performed by NASA Design and Analysis of Rotorcraft (NDARC). Aircraft are represented as a collection of components, with surrogate or semi-analytic models tuned to analysis and empirical correlations. The vehicle sizing rules, missions, and conditions are implemented in NDARC. NDARC performs fixed-point iterative solution procedures to find the vehicle design size. The most complete description of the concept aircraft is encapsulated in NDARC output files, which can be used to generate reports, transfer information to other tools, and used as the starting point for excursions and variant aircraft development. NDARC is capable of assessing the impact of advanced technology and design choices. NDARC calculates the economic measures, such as productivity, flyaway cost, and operating and support cost for the concept aircraft.

NDARC designs and analyzes a single concept aircraft at a time; excursions within a vehicle type are typically handled through a small number of changes to the design variables in the basic aircraft, while different vehicle types are designed with different basic aircraft as the input.

For a sized aircraft, NDARC calculates the weights and speeds to fly the noise metric conditions, as these are vehicle-specific, and must consider nonlinearities and limits in the propulsion system, not just aerodynamic performance (thus beyond the scope of the comprehensive analysis tool alone). NDARC calculate the airframe parasite and induced drag contributions which are used for trim in comprehensive analysis.

With the flexibility to evaluate many different types of vehicles with many different sizing rules, comes cost in terms of the amount of possible inputs available to the user: generally the number of input parameters varies inversely with the model fidelity. A large number of inputs (one hundred to several hundred) are generally needed to establish the definition of an aircraft and the sizing rules, but there are some convenience methods build into NDARC to allow the setup of some standard aircraft, and NASA has made its reference aircraft models available to NDARC users as templates for modification. At the present time, there are more than a dozen distinct types of aircraft available as NDARC examples, with numerous excursions and variants as well.

Setup of a functioning NDARC model for a new aircraft concept using these examples as guides takes a few days at most. Run time of an NDARC sizing job is typically on the order of tens of seconds, and subsequent performance cases run in no more than a few seconds. NDARC has a low memory footprint and is run on a typical personal computer.

For each of the aircraft in this demonstration, the text files defining the aircraft are about 200-400 lines in length. The run files, which define sizing rules, design missions and conditions, off-design missions and conditions, and restate the design variables, are typically on the order of 200 lines in length.

## CAMRAD II or CHARM

A comprehensive analysis code will simultaneously solve the rotor dynamics and aerodynamics for a trimmed or transient flight condition. NASA is not actively developing its own comprehensive analysis solution, and is instead applying commercial software for this step in the process. Two commercial codes, CAMRAD II and CHARM (Ref. 36), are being integrated interchangeably into the toolchain. For the present results, only CAMRAD II runs have been included.

By using two codes, it is hoped that a robust application programming interface can be defined which would allow other comprehensive analysis codes (*e.g.* RCAS, Ref. 37) to be integrated into the toolchain by a user of that software. Using two separate commercial codes will also allow comparisons to be made and some estimate of uncertainty to be established.

Both CAMRAD II and CHARM have well-validated free wake modeling capability. For interacting rotors, a freely convecting wake is necessary to accurately predict performance, and the lift+cruise, quadrotor, and side-by-side aircraft of this study all have rotors which interact to varying degrees in various stages of flight. A freely convecting wake which interacts with other blades on the same rotor and with blades on other rotors is essential to adequately predict the airloads on rotors when blade vortex interaction (BVI) is present, and especially if interacting rotor wakes are a factor. These BVI airloads can generate high noise and be the dominant noise source when present.

Similarly, for practical UAM rotors larger than a couple of feet in radius, elastic and kinematic motion should be considered to calculate the rotor trim and blade vortex interactions. Blade airloads and velocities will in general vary due to blade motion, induced velocity, and wake convection.

The two comprehensive analyses being integrated into the toolchain have different rotor aerodynamics and structural modeling approaches, which provides an opportunity to look at how those differences affect predicted noise. CAMRAD II has a lifting line representation of the rotor blades and wings, and therefore can only provide airloads at a discrete chordwise location, which can be used in a compact loading approximation. CHARM has the ability to treat the rotor blade and wings as either lifting lines or vortex panels, which allows noise to be calculated with a surface representation. CHARM uses a simpler structural representation than CAMRAD II and cannot calculate blade structural loads.

Whether or not the aerodynamic model of a comprehensive analysis code is adequate for evaluating the noise sources, a comprehensive analysis model of the structure is required. Building a comprehensive analysis model is generally a necessary step in the development of a meaningful high-fidelity simulation, as vehicle trim, rotor trim, and blade kinematic and elastic motion are usually computed by a comprehensive analysis which is coupled to CFD airloads. Therefore, comprehensive analysis is a necessary tool in the process and the work done here to integrate these tools can scale to more complex design processes. No standalone, uncoupled CFD will be of much value in evaluating rotorcraft noise in conceptual design.

A key benefit of a comprehensive analysis code is that the number of inputs are generally no greater than for NDARC, and often quite a bit less, with many of these inputs coming from a transliteration of the aircraft parameters from NDARC's output. Comprehensive analysis codes do require an outside analysis or experiment to provide airfoil section properties at all angles of attack for various Mach and/or Reynolds numbers; rotor kinematics due to articulation and control geometry; rotor blade equivalent beam properties. The two comprehensive analysis codes being integrated in the toolchain provide high-level rotor abstractions which simplify the input of the rotor properties for most common types of rotors, while maintaining the flexibility to build much more complex non-standard rotors if necessary. The run times of comprehensive analysis are generally in the tens of minutes for the cases, but more complex vehicles with multiple interacting rotors can take tens of hours on a personal computer. For the aircraft studied here, the memory requirements with interacting free wakes and small azimuthal resolution for acoustics became a limitation to running multiple simultaneous cases on a personal computer. The memory needs can also be problematic for going to a parallelized approach on high performance computing if the computing cluster's architecture does not provide large per-core memory efficiently.

The CAMRAD II aircraft description for the aircraft in this demonstration consists of text input files, with about 50 lines to describe the overall aircraft, and 50 lines for each of the rotors (more refined structural dynamic models mean more numbers, but not more quantities). These inputs describe the vehicle geometry, mass properties, and control strategy. The specification of the flight condition, modeling parameters for wakes, sensor/output settings, and a re-statement of the design variables are defined in a run file which is 100-200 lines long for each distinct run. Therefore, on the order of several hundred lines of input are required to describe the aircraft and conditions.

### AARON/ANOPP2

In order to predict the acoustic metrics for the present demonstration, a tool which predicts thickness, loading, and broadband noise sources, their propagation, and observer noise is necessary. The Aircraft NOise Prediction Program 2 (ANOPP2) and AeroAcoustic ROtor Noise (AARON) tools provide the acoustic calculations in the toolchain. AARON is the "user code" to perform rotorcraft calculations with ANOPP2. A Python script, "pyaaron," provides a simplified interface which is geared toward generating the certification noise and other typical rotorcraft calculations with a manageably small number of inputs, on the order of 20-50 lines.

For the type of elastic lifting line rotor representation that CAMRAD II employs, the AARON tool obtains the compact loading from CAMRAD II outputs, and applies a small number of supplemental inputs to calculate compact thickness (1 number per blade region) and self-noise (3 numbers per blade section). The supplemental inputs are defined at user-defined radial stations along the blade. Supplemental inputs are the airfoil maximum thickness-to-chord ratio along the blade for thickness noise; the section zero-lift angle, the

section trailing edge angle, and the section trailing edge thickness-to-chord ratio for self-noise. CAMRAD II or CHARM provides blade sectional position (aircraft position and rotor flapping, lag, pitch), Mach number, sectional load, and local angle of attack. The self-noise models have been based on simpler flow conditions than are likely to be present in UAM aircraft with multiple bodies and multiple rotors interacting, and until validation data becomes available, there will be some unknown uncertainty for these conditions.

For FAR Part 36 Subpart H Appendix H certification noise calculation (Ref. 38), AARON calculates the 1/3 octave spectrum at each point of a 19x19 hemisphere underneath the vehicle. This calculation is based on the CAMRAD II outputs and other supplemental information and includes both periodic sources (thickness and loading noise) and trailing edge self-noise. The following procedure is used separately for each of the three certification flight conditions: level flight, take off, and approach. Using the NDARC climb angle and speed as found in the CAMRAD II output, AARON translates the hemisphere through the certification flight track while computing acoustic metric time histories at 0.5 second intervals at each of the three certification microphone locations. From these acoustic metric time histories, AARON computes the Effective Perceived Noise Level (EPNL) [EPNdB] at each of the three certification microphones. The EPNL values at these three certification microphone locations, parsed from the AARON output, are then averaged to arrive at the single EPNL value for certification.

The calculation of noise for non-periodic or time-varying noise sources requires either a full time history calculation or some kind of equivalent quasi-periodic and quasi-stationary calculation. This is an area for future research, determining best practices and bounds of applicability are significant tasks and beyond the scope of the present demonstration. Time histories may need to be on the order of a minute of real-time, and therefore a very long calculation.

### RCOTOOLS

Rotorcraft Optimization Tools (RCOTOOLS, Ref. 39) is a set of Python libraries which serve as application wrappers for input/output and program execution of several tools. In this toolchain, RCOTOOLS interfaces for NDARC and CAMRAD II are used. The data connections depicted by gray lines in the XDSM diagrams of Figure 1 and Figure 2 are facilitated by RCOTOOLS. RCOTOOLS requires a Python platform to be installed along with some freely-available supporting packages, and may be executed on Linux, MacOS, and Windows platforms.

## TOOLCHAIN DEMONSTRATION

In order to test and demonstrate the toolchain, a set of four types of aircraft have been conceptually designed. These aircraft were designed to consistent design requirements for passenger payload and UAM mission. The demonstration is

an example of design paradigm A, "Design a distinct concept aircraft to a set of requirements."

The design mission is the same as that described in Ref. 40, with a 6 occupant payload flown on a 2-hop UAM sizing mission, depicted in Figure 13. The sizing mission provides vehicle size requirements due to energy and power requirements. The sizing mission has a vertical takeoff segment with hover out of ground effect, followed by a short vertical climb, a transition to cruise mode, and a climb to cruise altitude. For the aircraft examined here, the climb at 900 ft/min typically sizes installed power. The NDARC design methodology finds the minimum vehicle weight and power which will meet mission requirements by updating weight, vehicle size, power, and energy estimates until they are consistent and meet the requirements.

A set of design variables was identified for each aircraft type, selected for their anticipated impact on noise. A baseline aircraft for each type was defined, for reference of relative noise, weight, and performance changes.

As measures of performance, the design mission block time, flyaway cost, and vehicle empty weight are calculated by NDARC. For each metric of performance, lower magnitude is better. No attempt was made to develop an objective function, as weighting of the various noise, performance, and cost metrics, along with constraints on these metrics, is dependent on the particular design task. From these quantitative metrics however, many different objective functions may be developed.

To help establish practicality for conceptual design, the calculations were performed using personal workstation-type computers, and the resulting CPU/wall clock time and computer memory demands observed.

Noise metrics for the demonstration are defined as the 3 certification flight conditions of FAR Part 36 Subpart H Appendix H ("Appendix H", Ref. 38), expressed in EPNdB, which is the same as ICAO Annex 16 Volume I Chapter 8 (Ref. 41). While rotary-wing vehicles under 7,000 lb maximum takeoff weight can choose either Appendix J or Appendix H, Appendix H was selected for a number of reasons. Appendix H is more likely representative of annoyance, since it includes 3 separate conditions, any of which might pose difficulties with public acceptance. Many existing helicopters have certification noise data available (Ref. 42), including more than 45 distinct datapoints for helicopters under 7000 lb with Appendix H/Chapter 8 data. By developing the toolchain with capability to assess noise sources and propagation for Part 36 Appendix H conditions, it is hoped that other metrics may also be accurately predicted for relevant flight conditions.

Part 36 Subpart H Appendix H specifies three flight conditions, a "Takeoff," a "Flyover" ("Overflight" in EASA Chapter 8) and "Approach." For each condition, there are

three ground-based observers, and the measurements at these three observers are averaged to arrive at the certification value. The conditions specify flight path, speeds, and atmosphere. For Takeoff, the initial distance to the observer is specified, but vehicle speed and climb rate varies, so higher-performing vehicles may be further from the observer when overhead, potentially reducing observed noise. For Flyover, the altitude is constant but the speed varies between aircraft with vehicle performance. For Approach, the distance and descent angle are the same for all aircraft, but the speed varies between aircraft with vehicle performance. All vehicles are to be flown for certification at their maximum takeoff weight (WMTO).

The metric for Appendix H is in Effective Perceived Noise Level (EPNL), with calculation procedure specified in the regulations. EPNL attempts to regularize the perceived noise for each flight event by capturing human sensitivity to noise by frequency and by normalizing the duration of the perceived loudest portion of the event to a standard interval. As a result, a time history of sound levels needs to be simulated, and from this, a subset of the record will be used for the calculation of EPNL. This process makes it difficult to know *a priori* how long to simulate a non-periodic or non-stationary source, as the distance and orientation to observers vary. For periodic and stationary sources, only a single period need be analyzed, and this can be used to synthesize a time history.

A selection of technologies and design approaches known to reduce noise are enumerated below. Summaries of noise mitigation techniques for rotorcraft may be found in Refs. 1, 43, and 44 .

1. **Reduce rotor tip speed**: This reduces the intensity of many noise sources and may completely compressibility-related noise.
2. **Reduce rotor blade airfoil thickness**: reduces thickness noise due to displacement of air as the blades rotate.
3. **Sweep of rotor blade tip**: reduces or eliminates shock waves and may shift the location of tip vortices, reducing BVI.
4. **Droop (anhedral) of rotor blade tip**: shift the location of tip vortices, reducing BVI.
5. **Change aircraft trim (e.g. X-force or tilting)**: change relative location of vortices and blades, reducing BVI; changing rotor orientation may reduce observed noise due to directivity.
6. **Higher-harmonic- / individual-blade-control**: change loading and position of rotor blades, reducing BVI.
7. **Increase rotor blade count**: change loading and BVI; increase blade passage frequency
8. **Unequal rotor blade spacing**: spread energy and reduce peaks at fundamental frequencies
9. **Multiple rotor speeds among rotors**: spread energy out and reduce perceived tonal content

10. **Dissimilar blades**: change the relative position of vortices and blades to reduce BVI; spread energy and reduce peaks at fundamental frequencies
11. **Position blades away from other wakes/interference**: reduce or eliminate blade-wake-interaction noise
12. **Phase shift between rotors**: direct energy using interference to reduce observed noise
13. **Multi-element rotors (e.g. stacked rotors)**: change vortex convection to reduce BVI.
14. **Different blade count between rotors (avoid common multiples)**: spread energy to reduce peaks
15. **Reduce non-rotating structure interaction**: reduce noise generated on surfaces such as support booms or wings in close proximity to the rotors, often by increasing distance between rotor and structure
16. **Applying tubercles or serrations to leading or trailing edges**: reduce flow separation broadband noise, reduce BVI intensity by reducing the fast spanwise loading movement in a near-parallel BVI event
17. **Shielding of noise sources (including ducts)**: physically block the propagation of noise from source to observer
18. **Apply acoustic lining, muffling**: absorb or redirect sound near the source
19. **Introduce active phased interference**: reduce observed noise by using directivity and interference

Items 1 through 14 of these noise reduction technologies are at least partially addressable by the current approach. Item 15 may be addressed by the toolchain with the substitution of a different comprehensive analysis tool. Quantitative prediction of items 16 through 19 require additional capabilities to be added to the comprehensive analysis tools or, more likely, a coupled CFD solution.

Performance is defined as block speed or energy burn for the design mission. Cost for this demonstration is defined as either energy burn in the design mission or Harris-Scully flyaway cost (Ref. 5). Performance is block speed for the design mission or energy burn for the design mission.

## CONCEPT AIRCRAFT

Certain technologies and attributes which are expected to be included in a new-start aircraft have been included in the models for all of the concept aircraft. These features include muffling of the engine and drive system to reduce noise to a level lower than that of the rotor system, with associated weight and performance penalties, as discussed in Ref. 45. Systems weights include instrumented flight rules-capable avionics, cockpit controls, and fly-by-wire flight controls; these weights serve as the initial budget for an autonomous flight control system (see Ref. 46). Vibration mitigation weights have been included for each of the aircraft. Furnishings weights include crashworthy seats, sound dampening, and environmental control systems. The airframe and rotor structures use technology factors calibrated to

composite rotorcraft with crashworthiness considerations. The turboshaft engines represent state-of-the-art turboshafts, which at this scale are relatively fuel-thirsty and have not had much technology insertion for many decades. Further discussion of technologies for the concept aircraft may be found in Ref. 1.

In order to simplify the demonstration, the rotors for all of the concept aircraft are represented by rigid elements by ignoring blade elasticity. Rotor articulation is accommodated with flap, lag, and pitch elements. In general, for accurate noise prediction, elastic blades need to be modeled. The comprehensive analysis tools allow blade elasticity to be modeled, with CAMRAD II using a beam model and CHARM using mode shapes.

For each aircraft type, there is a baseline aircraft design with a set of baseline values for the design variables. For each set of design variables, the size, performance, and noise results may then be compared to the baseline. Values for baseline design variables are indicated in the design variable tables with **bold text**.

### Quiet Single Main Rotor Helicopter

The Quiet Single Main Rotor Helicopter (QSMR) aircraft type is representative of what would be possible with a state-of-the-art helicopter designed specifically for the UAM mission. In addition to shorter range, several design decisions have been made to bias toward low-noise. The tools in the toolchain have been validated with legacy helicopters, including some helicopters with the noise reduction technologies employed in this demonstration. Therefore, the predicted size, weight, performance, and noise of the QSMR is expected to be quite close to that of a real aircraft designed to these criteria and with the assumed level of technology. The relative predictions of the other vehicles can therefore be compared to the QSMR, in order to establish a reasonable expectation of the absolute merits and costs.

Traditional helicopters have tended to favor light weight and low installed power to reduce acquisition and operation costs. As with the other concept aircraft in this demonstration, the noise of the turboshaft and drive system is muffled, with a weight added to the aircraft. A depiction of a QSMR is provided in Figure 3. Key attributes are the muffled propulsion system and a NOTAR-style tailboom rather than a traditional tail rotor. The NOTAR system is heavier than a traditional tail rotor, but can reduce the anti-torque contribution to noise to such an extent that the main rotor is by far the dominant noise source. A more complete description of the basic QSMR aircraft and its design philosophy is presented in Ref. 45.



**Figure 3. Rendering of a QSMR concept aircraft**

The design variables for the QSMR are listed in Table 1. As main rotor tip speed is varied, the design $C_W/\sigma_T$ (aircraft design gross weight coefficient divided by rotor thrust-weighted solidity) was kept constant. The number of rotor blades were incremented or decremented in order to approximately maintain a blade aspect ratio as solidity varied, hence shown in italic font. The baseline rotor speed is 600 ft/s. The tip droop location is the rotor blade nondimensional spanwise station (0 at root, 1 at tip) at which a change in blade dihedral is introduced, with the outboard portion of the blade having a constant droop angle, positive downward, with the baseline being no droop. Higher-harmonic control (HHC) is given as the amplitude of pitch input at a frequency of 2/rev and whichever phase angle is seen to have the greatest reduction in noise.

**Table 1. QSMR design variables**

| Design Variable | Values (**reference in bold**) | | | | | | |
|---|---|---|---|---|---|---|---|
| Main rotor tip speed, ft/s | 400 | 450 | 500 | 550 | **600** | 650 | 700 |
| *(number of blades)* | *8* | *6* | *6* | *4* | *4* | *3* | *3* |
| Tip droop location, r/R | 0.90 | 0.94 | **1.0** | | | | |
| Tip droop, deg | **0** | 10 | 20 | 30 | | | |
| HHC pitch, deg | **0** | 1 | 2 | | | | |

### Quadrotor

The quadrotor aircraft is depicted in Figure 4. The quadrotor is intended to represent multirotor-type aircraft which use collective or rotor speed control for flight control, without cyclic control. The basic quadrotor aircraft model was first described in Ref. 46, with more discussion in Ref. 29. For the demonstration, only single-tip-speed, collective-controlled excursions were used, for the reasons mentioned above regarding variable-speed rotor noise calculations still requiring developmental work.

**Figure 4. Rendering of a quadrotor concept aircraft**

One interesting attribute of the designs for the NASA quadrotor concept aircraft is that the rear rotors are mounted higher on the aircraft than the forward rotors, as shown in Figure 5. Initial design work with the free wake comprehensive analysis in CAMRAD II (Ref. 26) led to this design decision, as a significant reduction in power required for cruise was predicted. Subsequent higher fidelity analysis, documented in Ref. 27, has confirmed the beneficial effect, albeit with a different magnitude.



**Figure 5. Quadrotor rear rotor vertical placement**

The design variables for the quadrotor are listed in Table 2. Rotor tip speed is the tip speed of all of the rotors, as the tip speed is synchronized among all of the rotors. The number of blades, as before, varies with solidity to maintain blade aspect ratio, and the number of blades is the number of blades per rotor, such that the total number of blades is 4 times the number of blades in the table. The rotors are locked in phase relative to each other, such that rotor blade *i* is at zero azimuth at the same instant for all blades. The right-front and left-rear rotors turn counterclockwise, and the left-front and right-rear rotors turn clockwise. Tip droop is defined in the same manner as for the QSMR. The rear rotor height parameter is the water line location of the rear rotor relative to the front rotor normalized by rotor radius, for the aircraft in its nominal zero-pitch attitude. In flight, the vehicle trim will change the relative position of the two rotors.

**Table 2. Quadrotor design variables**

| Design Variable | Values (**reference in bold**) | | | | | | | |
|---|---|---|---|---|---|---|---|---|
| Rotor tip speed, ft/s | 375 | 400 | 450 | 500 | **550** | 600 | 650 | 700 |
| *(number of blades)* | 7 | 6 | 5 | 4 | 3 | 3 | 3 | 3 |
| Tip droop location, r/R | 0.90 | 0.94 | **1.0** | | | | | |
| Tip droop, deg | **0** | 10 | 20 | 30 | | | | |
| Rear rotor height, Δz/R | **0.45** | 1.05 | | | | | | |

## Lift+Cruise Aircraft

The Lift+Cruise aircraft was initially described in Ref. 46, and is essentially a stopping-rotor thrust- and lift-compound aircraft. The basic vehicle is depicted in Figure 6. There are three distinct flight modes for the aircraft: helicopter mode with the lifting rotors turning, compound mode with lifting and thrusting rotors operating, and airplane mode with the lifting rotors stopped and aligned with the blade axis pointed along the vehicle longitudinal axis, and therefore nominally aligned with the free stream to minimize drag. Unlike the other aircraft in this demonstration, the lift+cruise aircraft can only have two blades on the lifting rotors, so as the rotor speed and solidity changes, no change is allowed in number of blades. The vast majority of lift+cruise aircraft being proposed have fixed pitch, but for this demonstration, single tip-speed collective control without cyclic is used for all lifting rotors. A separate tip speed is used for the pusher rotor.
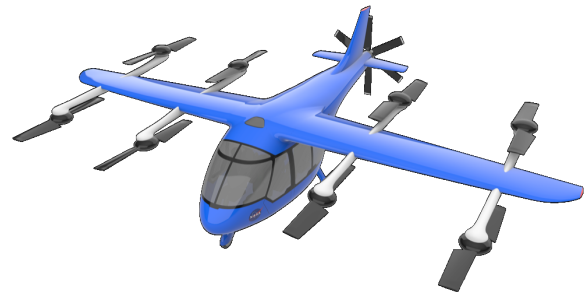


**Figure 6. Rendering of lift+cruise aircraft**

Similar to the quadrotor, the lift+cruise aircraft has the rear rotors mounted higher than the front rotors. The performance effects are similar for rotor-rotor interference, but there are now two additional considerations: the influence of the boom for an under-mounted rotor, and the interference with the wing. By placing the front rotor under the support boom, a simpler and more compact support can be built.

The design variables for the lift+cruise aircraft are listed in Table 3. Main rotor tip speed is the tip speed of all of the rotors, as the tip speed is synchronized among all of the rotors. The number of blades is fixed at 2 and is the number of blades per rotor, such that the total number of blades is 16, plus the 6 blades in the pusher rotor. The rotors are locked in phase relative to each other, such that rotor blade *i* is at zero azimuth at the same instant for all blades. The right-front and left-rear rotors turn counterclockwise, and the left-front and right-rear rotors turn clockwise. Tip droop is defined in the same manner as for the QSMR. The rear rotor height parameter is the water line location of the rear rotor relative to the front rotor normalized by rotor radius, for the aircraft in its nominal zero-pitch attitude. In flight, the vehicle trim will change the relative position of the two rotors, and because there are more controls than degrees of freedom, pitch attitude is a degree of freedom which may be specified when operating in compound mode.

Figure 7 depicts the height definition, with positive upward, and the rotor shown at a baseline height position.
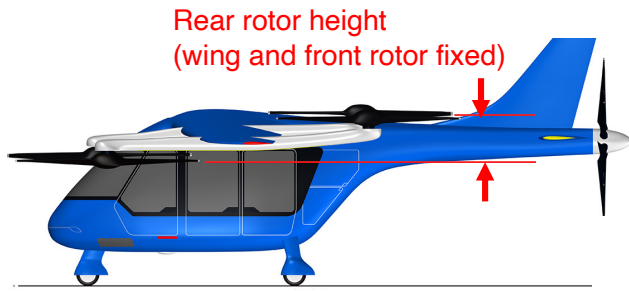


Figure 7.  Lift+Cruise rear rotor height

**Table 3. Lift+Cruise design variables**

| Design Variable | Values (**reference in bold**) | | | | | | |
|---|---|---|---|---|---|---|---|
| Main rotor tip speed, ft/s | 400 | 450 | 500 | **550** | 600 | 650 | 700 |
| (number of blades) | 2 | 2 | 2 | 2 | 2 | 2 | 2 |
| Tip droop location, r/R | 0.90 | 0.94 | **1.0** | | | | |
| Tip droop, deg | **0** | 10 | 20 | 30 | | | |
| Rear rotor height, Δz/R | **0.45** | 1.05 | | | | | |

Not examined in this demonstration, but worthy of discussion as a capability which will be added to the toolchain, are the design options with regard to the front rotors. The noise of a rotor in proximity to a fixed support has been examined recently in experiments and high-fidelity computation (Ref. 47), and the noise is expected to be greater for a rotor mounted underneath a nearby support than above it. The mechanism for this greater noise is largely because of the low-pressure blade passing near the surface of the boom and the boom surface radiating the noise from a relatively large area. Predicting this boom-interference effect is not possible with one of the comprehensive analyses in the toolchain (CAMRAD II), but may be possible with the other (CHARM). For the present demonstration, the boom interference effect is neglected for both front and rear rotors.

Additionally, the rotor wake can be expected to remain under the wing at all times during forward flight, instead of potentially impinging on the wing. The noise and moreover, performance of the wing should be better without the turning- or stopped-rotor wake impinging on it. A rapid and non-linear change in trim would be expected when the rotor wake from a turning rotor suddenly impinged on a wing as flight conditions changed.

**Side-by-Side Helicopter**

The side-by-side helicopter is representative of a high-performance helicopter, which has main rotors which intentionally interact as they physically overlap and intermesh. The side-by-side aircraft is depicted in Figure 8, with a support cross-bar to hold the rotors up, but not

generating significant lift. The interaction of the main rotors is intended to reduce induced power in forward flight. The NASA side-by-side aircraft has been described in Refs.18, 28, 29, and 46.



Figure 8. Rendering of a side-by-side helicopter

For all instances of the side-by-side aircraft in this demonstration, the relative rotor phasing is held constant, the rotors are articulated, there are 4 blades per rotor, and the rotors are controlled via collective and cyclic pitch.
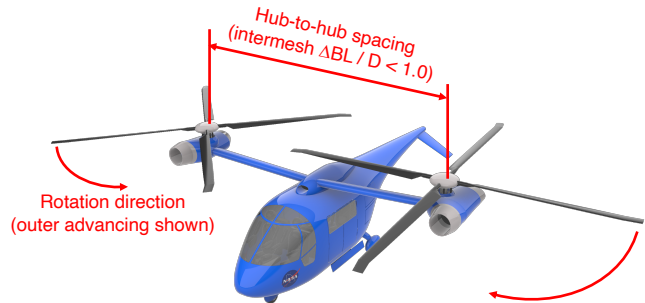


Figure 9. Side-by-Side rotor spacing, direction of rotation

The design variables for the side-by-side aircraft are shown in Table 4. In addition to the types of design variables in the other vehicles, the rotor-hub spacing as a fraction of diameter and the direction of rotation have been added. The rotor direction of rotation is the only discontinuous design variable examined; all of the other design variables have been continuous-valued.

**Table 4. Side-by-side design variables**

| Design Variable | Values (**reference in bold**) | | | | | | |
|---|---|---|---|---|---|---|---|
| Main rotor tip speed, ft/s | 400 | 450 | 500 | **550** | 600 | 650 | 700 |
| (number of blades) | 4 | 4 | 4 | 4 | 4 | 4 | 4 |
| Tip droop location, r/R | 0.90 | 0.94 | **1.0** | | | | |
| Tip droop, deg | **0** | 10 | 20 | 30 | | | |
| HHC pitch, deg | **0** | 1.5 | 2 | | | | |
| Hub-to-hub spacing (ΔBL / D) | 0.75 | **0.85** | 0.95 | 1.05 | | | |
| Direction of rotation | **Outboard advance** | | Outboard retreat | | | | |

## SELECTED RESULTS

For the demonstration, many design variables have been exercised and compared for the 4 types of aircraft. This section will present some of the more interesting observations. Bold values in the results tables are the greatest improvement (lower is better) for a particular metric among the tabulated values, and the underlined value is the reference design variable value.

**Varying design tip speed**

The aircraft in this demonstration all have relatively high takeoff performance, due to the 900 ft/min (274 m/min) climb rate requirement in the design mission applied to all of the aircraft designs. This resulted in a higher installed power, so that for the takeoff noise certification condition, the aircraft is both further from the observer than for existing helicopters and the rotor is operating with a quickly convecting wake. These two effects combine to reduce the noise for the QSMR, quadrotor, and side-by-side by at least 10 EPNdB compared to helicopters of similar weight, as seen in Figure 14(a). The colors and markers are consistent in the figures, with QSMR a yellow circle, quadrotor a blue square, lift+cruise a red triangle, and side-by-side a purple diamond. The lift+cruise in compound mode trim is the loudest and heaviest of the vehicles, due in large part to the high number of rotors, rotor-rotor interactions, and operating at a higher loading due to the rotor radius being constrained to no more than 5 ft (1.524 m).

Flyover results with varying rotor tip speed are shown in Figure 14(b). for the QSMR, quadrotor, and side-by-side are also in general quieter than existing helicopters, while the lift+cruise is once again similar to existing helicopters.

Approach results for varying rotor tip speed are shown in Figure 14(c). Approach noise is close to existing helicopters if the tip speeds are at the higher end of the range of speeds examined, but noise quickly reduces as tip speed goes to the lower end of the range. The lowest tip speed, of 375 ft/s for the quadrotor, does not improve the approach noise or the flyover noise compared to the 400 ft/s case.

Vehicle flyaway cost generally increases with rotor tip speed reduction as shown in Figure 15 and the vehicle-specific tables. The increase in cost with reducing tip speed is not always accompanied by a reduction in noise, and this trade is likely to be of importance in UAM conceptual design.

Tip speed reduction is a powerful tool to reduce noise for most aircraft and in most conditions, but the Flyover condition for the aircraft in this demonstration is illustrative of the necessity of quantitative calculation in conceptual design. For the QSMR (Figure 16 and Table 6), the reduction in rotor speed is quite effective at reducing noise until 500 ft/s, and ineffective below that tip speed. Figure 17 presents the

quadrotor noise and weight compared to existing helicopters, with tabulated results of the quadrotor in

Table 7. The trend with tip speed is favorable for all three conditions, until 400 ft/s tip speed. The Flyover case is interesting, as the quadrotor improves for some lower tip speeds, but is slightly worse for others. Reducing tip speed from 550 ft/s to 375 ft/s would cost +0.2 dB in EPNL, +9% in empty weight, +18% in mission block time, and +14% in flyaway cost.

The lift+cruise aircraft is isolated in Figure 18 and Table 8, and the noise is seen to be similar to existing helicopters. The weight of the lift+cruise aircraft is also significantly larger than that of the other aircraft. Reducing tip speed only has limited improvement.

The side-by-side set of noise and gross weight charts with varying tip speed are in Figure 19, and the trend is complicated by the Flyover behavior. For the side-by-side, the noise is generally lower at higher tip speeds. If flyover noise reduction is the goal, then some other approach should be considered rather than tip speed variation. The loading noise is a big part of the noise for this case, and so applying droop and/or higher-harmonic control may reduce this noise. Figure 20 shows the loading over the disk (lighter colors higher load) for the baseline, drooped, and higher-hamonic pitch control cases. The noise with droop is reduced by 1.7 EPNdB, and the blade-vortex-interaction events on the advancing side are reduced. Loading is increased at the advancing side tip as well. For the HHC case, a reduction of 1.2 EPNdB is possible with 1 degree of 2/rev excitation, and reductions are seen in the BVI events (light-colored stripes) without increasing the loading at the tip. Interestingly, the overlap region (270 degrees, left side of the disk in the image) does not seem to be very prominent for the side-by-side, so it is not contributing much loading noise during Flyover.

The side-by-side approach results show a reduction in advancing-side and retreating-side BVI event intensity with reducing tip speed, shown in Figure 21, where the visible radial stripes in loading are BVI events. This difference in retreating-side phenomena between flyover and approach opens up opportunities to consider variable-geometry or selective trim and HHC input to maintain high cruise efficiency in cruise and give up performance on approach for lower noise. These new directions for design excursions are beyond the scope of the demonstration, but possible with the toolchain.

**Rotor-to-Rotor interference**

The effects of rotor position and the methods for calculating rotor-rotor interference are important to understand in order to improve noise. The lift+cruise aircraft has the most rotor-rotor interactions, and therefore it makes an interesting test case for the effects of trim and modeling. Table 5 illustrates some variations for the lift+cruise aircraft in the Approach condition. The baseline aircraft noise is calculated with zero pitch attitude on the -6 degree descent, and with fully coupled

free wakes from the 9 rotors (8 lift + 1 pusher), and is believed to represent the most accurate solution via the toolchain.

The first comparison is to a different trim state, with the nose pitched down 6 degrees, and also calculated with fully coupled free wakes. The noise is seen to be reduced by 3.8 EPNdB, and this is likely a realizable improvement.

The second change is to raise the rear rotors by 3 feet (from $\Delta Z/R$ of 0.45 to 1.05), keeping pitch at 0 degrees as in the baseline, and using fully coupled free wakes. In this case, a reduction of 1.3 EPNdB is predicted, and this is also likely to be a realizable improvement.

**Table 5. Lift+Cruise trim and modeling effects on approach noise**

|  | Level (EPNdB) | Δ (EPNdB) |
|---|---|---|
| Baseline, 550 ft/s approach | 87.7 | -- |
| Pitch -6 deg | 83.8 | -3.8 |
| $\Delta Z=1.05R$ | 86.4 | -1.3 |
| No rotor-rotor interference | 84.3 | -3.3 |
| Separate wake geometries | 87.7 | 0.0 |
| No pusher noise | 87.5 | -0.1 |

If all rotor-rotor interference is ignored and each rotor only sees its own influence, then a 3.3 EPNdB reduction is observed. This reduction is not realizable in practice, but shows the importance of rotor-rotor interaction to the noise.

If all of the rotors interfere with each other, but the wake geometries are not fully coupled, then no difference is observed. This is helpful from a computational demand standpoint, but more work is necessary to determine the bounds of validity for this approach.

Finally, ignoring the pusher noise shows that the overall noise is indeed dominated by the lifting rotors. This noise reduction is again not realizable, but does hint at a design and operation trade. The best mode for flying approach is probably to fly in airplane mode as long as possible, but the stall boundary and lift rotor transients need to be modeled in order to determine the safe flight corridor. Since the intent of this demonstration is to exercise the toolchain, not to design the "best" aircraft or set the optimal operating schedule, minimizing approach noise was not pursued at this time.

### Computation Resources

The time and computation resources required to execute the toolchain are important considerations to determine whether or not this process is compatible with conceptual design. The NDARC sizing and analysis cases run in less than a minute, but the comprehensive analysis and noise calculations can take tens or minutes to tens of hours on a workstation. The comprehensive analysis tools are not currently parallelized, but the noise tools AARON/ANOPP2 are. Two aircraft cases are presented here as representative timing cases. The

quadrotor and side-by-side were both evaluated with fully interacting (intra-rotor and rotor-to-rotor) free wakes. Only minor adjustments were made to tune the run cases; with more effort, the convergence of loops in the solution of the comprehensive analysis could be sped up significantly, but no single set of parameters is likely to speed up all cases.

The quadrotor cases took much longer to run than the side-by-side case, with the quadrotor shown in Figure 10. The number of blades is shown visually on the graphic to illustrate the strong dependence on number of blades. The number of blades is likely just one factor in the run time, as the flyover case shows a significant computation time increase with reducing tip speed even for cases with the same number of blades. For the reference case of 550 ft/s tip speed, the takeoff and approach computations each ran in about 1 hour, with flyover running in about 3.7 hours. Each case can be run independently, allowing an "embarrassingly parallel" or "embarallel" execution of the calculations for the toolchain. The memory required for the quadrotor was also an important consideration, and was a limitation on the ability to run embarallel cases, as CAMRAD II used up to 13 GB of RAM for the 7-bladed rotor cases. The peak memory usage was at the end of the calculation, for a relatively short period of time of a few minutes as CAMRAD II performed "post-trim" wake calculations with a finer azimuth step of 1.5 degrees to generate data for the noise calculations. Thus, with a combination of operating system memory management and inherent staggering of peak memory demands, simultaneous runs of the three certification conditions was run on an 8-core 16 GB machine with only minor slowdown in CPU time compared to the three cases run sequentially. Running more than 3 cases simultaneously resulted in more virtual memory usage, which slowed down computations.
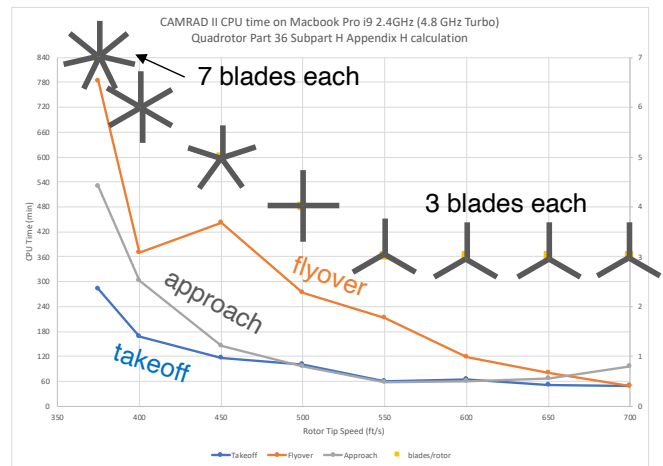


**Figure 10. CAMRAD II run timing for the quadrotor**

Compared to the quadrotor, the side-by-side comprehensive analysis cases were run very quickly. To illustrate the relative time, the side-by-side timing is shown with the same vertical time scale as the quadrotor in Figure 11.
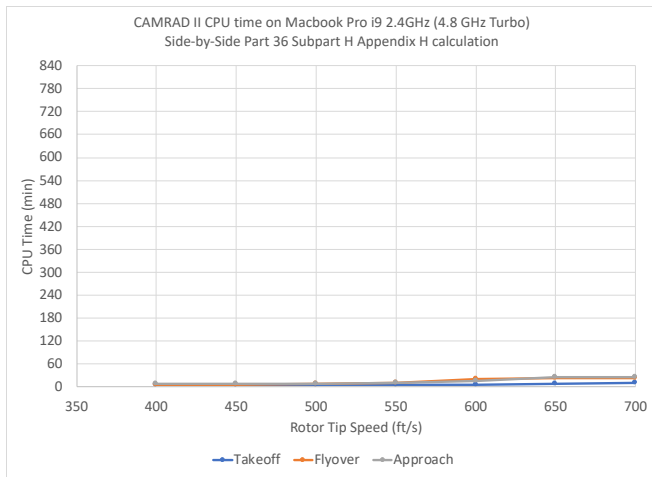
**Figure 11. CAMRAD II run timing for side-by-side, same time scale as quadrotor**

The side-by-side helicopter run time shows a different trend with tip speed, as evident in Figure 12. Since the number of blades was constant at 4 blades per rotor, the effect is likely due to some combination of advance ratio and rotor interaction causing greater evaluation time in the circulation, trim, and wake geometry loops. The magnitude of the computation time difference between the different tip speeds is interesting, but not expected to be problematic, as many runs can still be executed in the course of a day. The memory demands for the 2x 4-bladed rotors are about half of the memory demands of the quadrotor, allowing up to 6 simultaneous executions (2 excursions at a time, each running 3 certification conditions) with little parallelization slowdown on an 8-core, 16 GB random-access memory (RAM) machine.
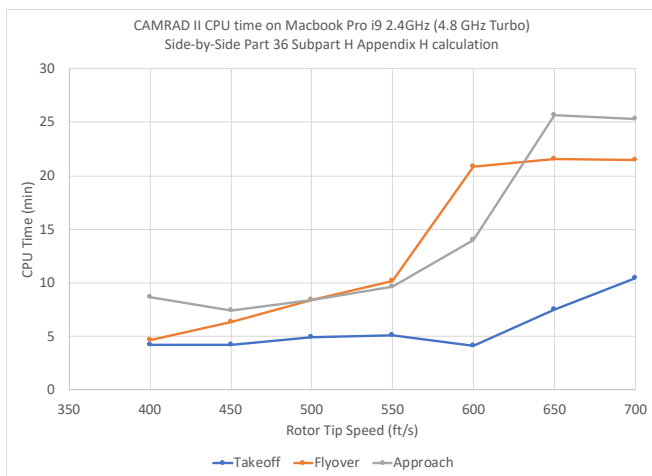


**Figure 12. CAMRAD II run timing with tip speed for side-by-side, expanded scale**

In the course of performing this demonstration, a few software bugs were discovered, requiring minor modifications to CAMRAD II, ANOPP2, and pyaaron. Some convenience features were added to RCOTOOLS to parse

results. The toolchain was able to perform these calculations on MacOS, Windows, and Linux computers, including both workstations and a Linux supercomputer.

## CONCLUSIONS

The toolchain in this demonstration is capable of quantitatively trading several relevant noise reduction technologies and design approaches for aircraft which can perform the Urban Air Mobility mission. While rotor tip speed reduction does indeed usually reduce noise, the toolchain is capable of determining the cost of this speed reduction, and also determine when speed reduction no longer improves noise. The calculations performed for these trades are quick enough to allow several simultaneous aircraft types to be evaluated by an individual designer or design team, with the calculations performed on workstation computers.

The four vehicle types examined in the demonstration have some variation in the relative effectiveness of noise reduction approaches, and sometimes display divergent trends. Using the three certification conditions of Appendix H rather than a single flyover point from Appendix J may help prevent unintended consequences of optimization. The noise levels predicted for the aircraft vary from similar to the existing rotorcraft fleet to tens of EPNdB quieter.

Future work will focus on the limitations of the current process. The toolchain cannot presently evaluate the noise for vehicles where the rotors have varying tip speeds such that no periodic or quasi-periodic solution can be found. This toolchain cannot presently address several important sources of noise nor some known noise reduction approaches. There are also uncertainties with regards to the best way to assess vehicles with variable rotor speed for trim and control, as the assumptions of periodic and stationary-in-time noise sources may be invalid.

## NOTATION

| | |
|---|---|
| $\rho$ | Air density |
| $\sigma_T$ | Thrust-weighted solidity |
| BVI | Blade-vortex-interaction |
| $C_W$ | Weight coefficient, $W/\rho A V_{tip}^2$ |
| EPNdB | Effective perceived noise level, in decibels |
| EPNL | Effective perceived noise level |
| HHC | Higher-harmonic control |
| QSMR | Quiet single main rotor helicopter |
| WMTO | Maximum takeoff weight |

## REFERENCES

1. Antcliff, K. Whiteside, S., Silva, C. and Kohlman, L., "Baseline Assumptions and Future Research Areas for Urban Air Mobility Vehicles," AIAA-2019-0528, AIAA SciTech Forum, January 2019.
2. Rabe, D., and Wilke, G., "Parametric Design Studies of the Helicopter Rotor Noise using Variable-Fidelity

Methods," AHS International 74th Annual Forum & Technology Display, Phoenix, Arizona, USA, May 2018.

3. Boyd, D., Greenwood, E., Watts, M., Lopes, L., "Examination of a Rotorcraft Noise Prediction Method and Comparison to Flight Test Data," NASA-TM-2017-219370

4. [Johnson, W., "A Quiet Helicopter for Air Taxi Operations," VFS Aeromechanics for Advanced Vertical Flight Technical Meeting, San Jose, CA, January 2020.

5. Johnson, W. "NDARC — NASA Design and Analysis of Rotorcraft. Validation and Demonstration." American Helicopter Society Specialists' Conference on Aeromechanics, San Francisco, CA, January 2010.

6. Johnson, W., "Technology Drivers in the Development of CAMRAD II," American Helicopter Society Aeromechanics Specialist Meeting, San Francisco, California, January 1994.

7. Johnson, W. "Rotorcraft Aeromechanics Applications of a Comprehensive Analysis." HeliJapan 1998: AHS International Meeting on Rotorcraft Technology and Disaster Relief, Gifu, Japan, April 1998.

8. Johnson, W. "Rotorcraft Aerodynamic Models for a Comprehensive Analysis." American Helicopter Society 54th Annual Forum, Washington, D.C., May 1998.

9. Lopes, L., Burley, C., "Design of the Next Generation Aircraft Noise Prediction Program: ANOPP2,"AIAA-2011-2854 17th AIAA/CEAS Aeroacoustics Conference, Portland, Oregon, June 2011.

10. Moorman, R., "Noise in the Cities—Revisited," *VERTIFLITE*, November/December 2016.

11. Torenbeek, E., *Advanced Aircraft Design: Conceptual Design, Technology and Optimization of Subsonic Civil Airplanes*, Wiley, 2013.

12. Raymer, D., *Aircraft Design, A Conceptual Approach, 6th ed.*, AIAA Education Series, Reston, Virginia, 2018.

13. Nicholai, L., and Carichner, G., Fundamentals of Aircraft and Airship Design, Vol. 1, AIAA Education Series, Reston, Virginia, 2010.

14. Roskam, J., *Airplane Design, Parts I-VIII Digital Edition*, DARCorporation, Lawrence, Kansas, 2018.

15. Gudmundsson, S., *General Aviation Aircraft Design: Applied Methods and Procedures*, Elsevier, 2014.

16. Sinsay, J., "Re-imagining Rotorcraft Advanced Design," Rotorcraft Virtual Engineering Conference, Liverpool, U.K., November 2016.

17. Russell, C. and Basset, P.-M., "Conceptual Design of Environmentally Friendly Rotorcraft – A Comparison of NASA and ONERA Approaches," 71st AHS Annual Forum, Virginia Beach, Virginia, May 2015.

18. Silva, C., Johnson, W., and Solis, E., "Multidisciplinary Conceptual Design for Reduced-Emission Rotorcraft," AHS Technical Meeting on Aeromechanics Design for Vertical Lift, San Francisco, California, January 2018.

19. Sridharan, A. and Govindarajan, B., "Evaluation of Sizing Strategies for eVTOL UAV Configurations," Vertical flight Society's 76th Annual Forum and Technology Display, October 2020 (Virtual event).

20. Gray, J., Hwang, J., Martins, J. R. R. A., Moore, K., and Naylor, B., "OpenMDAO: An Open-Source Framework for Multidisciplinary Design, Analysis, and Optimization," Structural and Multidisciplinary Optimization, 2019.

21. Kim, H., Malone, B., Sobieszczanski-Sobieski, J., "A Distributed, Parallel, and collaborative Environment for Design of Complex Systems," AIAA-2004-1848, 45th AIAA/ASME/ASCE/AHS/ASC Structures, Structural Dynamics, and Materials Conference, Palm Springs, California, April 2004.

22. Hwang, J., and Martins, J. R. R. A., "A computational architecture for coupling heterogeneous numerical models and computing coupled derivatives," ACM Transactions on Mathematical Software, 44(4):Article 37, 2018.

23. Multiple authors, "Publications | OpenMDAO.org," http://openmdao.org/publications/, accessed April 2021.

24. Potsdam, M., and Strawn, R., "CFD Simulations of Tiltrotor Configurations in Hover," American Helicopter Society 58th Annual Forum, Montreal, Quebec, Canada, June 2002.

25. Cadieux, F., Barad, M., Jensen, J., and Cetin, K., "Predicting Quadcopter Noise with the Lattice-Boltzmann Method," AIAA-2020-, AIAA AVIATION 2020, (Virtual event), June 2020. (NASA Technical Report Server ID 20200011494).

26. Johnson, W., Silva, C., and Solis, E., "Concept Vehicles for VTOL Air Taxi Operations," AHS Technical Meeting on Aeromechanics Design for Vertical Lift, San Francisco, California, January 2018.

27. Ventura Diaz, P. and Yoon, S., "Computational Study of NASA's Quadrotor Urban Air Taxi Concept," AIAA-2020-0302, AIAA SciTech Forum, Orlando, Florida, January 2020.

28. Ventura Diaz, P., Johnson, W., Ahmadz, J., and Yoon, S.," The Side-by-Side Urban Air Taxi Concept," AIAA Aviation Forum 2019, Dallas, Texas, June 2019.

29. Johnson,, W. and Silva, C., "Observations from Exploration of VTOL Urban Air Mobility Designs," 7th Asian/Australian Rotorcraft Forum, Jeju Island, Korea, October 30–November 1, 2018.

30. Thomas, G., Chapman, J., Fuzaro Alencar, J., Hashmatullah, H., Sadey, D., and Csank, J., "Multidisciplinary Systems Analysis of a Six Passenger Quadrotor Urban Air Mobility Vehicle Powertrain," AIAA-2020-3564, AIAA Propulsion and Energy 2020 Forum, August 2020.

31. Malpica, C. and Withrow-Maser, S., "Handling Qualities Analysis of Blade Pitch and Rotor Speed Controlled eVTOL Quadrotor Concepts for Urban Air Mobility" VFS International Powered Lift Conference 2020, San Jose, CA, January 2020.

32. Withrow–Maser, S., Malpica, C., Nagami, K., "Multirotor Configuration Trades Informed by Handling Qualities for Urban Air Mobility Application " Vertical Flight Society's 76th Annual Forum & Technology Display, October 2020 (Virtual event).

33. Lucia, D., "The SensorCraft Configurations: A Non-Linear AeroServoElastic Challenge for Aviation," AIAA-2005-1943, 46th AIAA/ASME/ASCE/AHS/ASC Structures, Structural Dynamics, & Materials Conference, Austin, TX, April 2005.

34. Martinez, J., Flick, P., Perdzock, J., Dale, G., Davis, M., "An Overview of SensorCraft Capabilities and Key Enabling Technologies," AIAA-2008-7185, 26th AIAA Applied Aerodynamics Conference, Honolulu, HI, August 2008.

35. Schrage, D., "Technology for Rotorcraft Affordability Through Integrated Product/Process Development (IPPD)," American Helicopter Society 55th Annual Forum and Technology Display, Montreal, Quebec, Canada, May 1999.

36. Wachspress, D., "Continuum Dynamics, Inc: eVTOL Aircraft Modeling and Simulation," 8th Annual Electric VTOL Sympoosium, January 2021.

37. Saberi, H. and Ormiston, R., "Overview of RCAS and Application to Advanced Rotorcraft Problems," AHS 4th Decennial Specialist's Conference on Aeromechanics, San Francisco, California, January 2004.

38. United States Code of Federal Regulations, "PART 36—NOISE STANDARDS: AIRCRAFT TYPE AND AIRWORTHINESS CERTIFICATION," Title 14, Chapter I, Subchapter C, Part 36.

39. Meyn, L., "Rotorcraft Optimization Tools: Incorporating Rotorcraft Design Codes into Multi-Disciplinary Design, Analysis, and Optimization," AHS Technical Meeting on Aeromechanics Design for Vertical Lift, San Francisco, CA, January 2018.

40. Patterson, M., Antcliff, K., and Kohlman, L., "A Proposed Approach to Studying Urban Air Mobility Missions Including an Initial Exploration of Mission Requirements," AHS International 74th Annual Forum & Technology Display, Phoenix, Arizona, May 2018.

41. Anon., "Annex 16 - Environmental Protection - Volume I - Aircraft Noise, 8th Edition," International Civil Aviation Organization, July 2017.

42. Anon., "Rotorcraft noise database, Issue 35, European Union Aviation Safety Agency, 25 March 2021, retrieved April 2021 from https://www.easa.europa.eu/domains/environment/easa-certification-noise-levels.

43. Johnson, W., *Rotorcraft Aeromechanics*, Cambridge University Press, New York, 2013.

44. ICCAIA: Snecma, Airbus Helicopters, Sikorsky Aircraft, Bell Helicopter, AgustaWestland, Turbomeca, Marenco Swisshelicopter; Research Centers: NASA, DLR, ONERA, JAXA, "Helicopter Noise Reduction Technology: Status Report," International Civil Aviation Organization, April 2015.

45. Johnson, W., "A Quiet Helicopter for Air Taxi Operations" VFS Aeromechanics for Advanced Vertical Flight Technical Meeting, San Jose, California, January 2020.

46. Silva, C., Johnson, W., Antcliff, K.R., and Patterson, M.D., "VTOL Urban Air Mobility Concept Vehicles for Technology Development," AIAA 2018-3847, 2018 Aviation Technology, Integration, and Operations Conference, AIAA Aviation Forum, Dallas, Texas, June 2018.

47. Zawodny, N., and Boyd, D., "Investigation of Rotor-Airframe Interaction Noise Associated with Small-Scale Rotary-Wing Unmanned Aircraft Systems," AHS 73rd Annual Forum, FortWorth, Texas, May 2017.
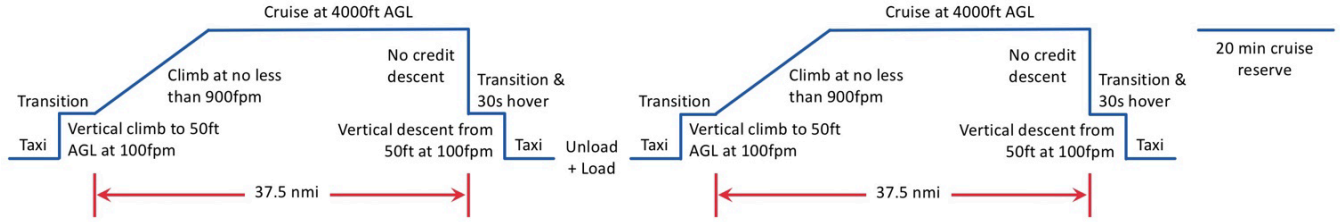
# FIGURES



**Figure 13. UAM design mission profile**
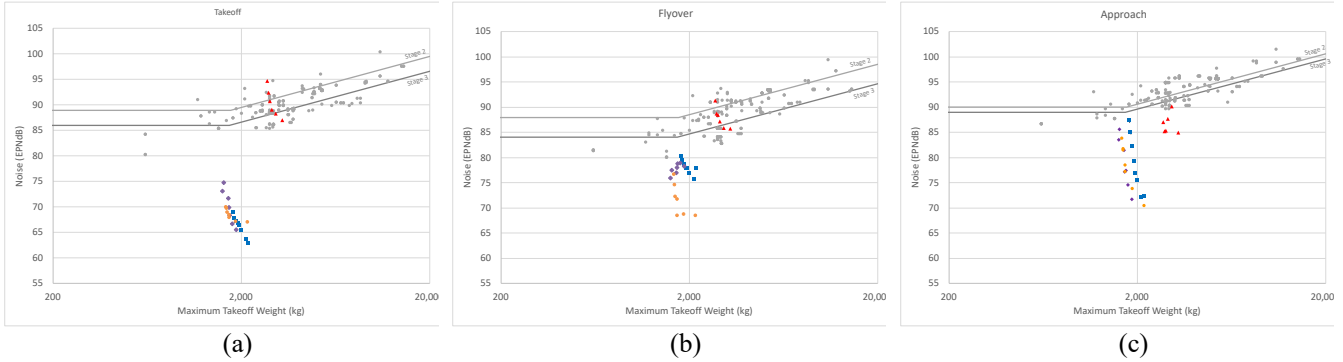


| (a) | (b) | (c) |
|---|---|---|

**Figure 14. Noise and max gross weight for the 4 types of aircraft with varying tip speed compared to existing helicopters (QSMR yellow circle, quadrotor blue square, lift+cruise red triangle, side-by-side purple diamond)**



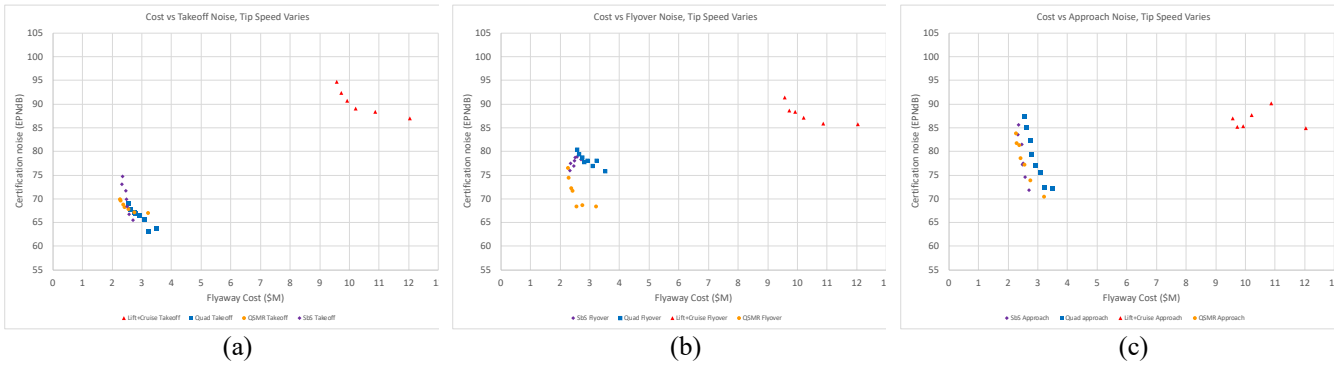| (a) | (b) | (c) |
|---|---|---|

**Figure 15. Noise and flyaway cost for the 4 types of aircraft with varying tip speed (QSMR yellow circle, quadrotor blue square, lift+cruise red triangle, side-by-side purple diamond)**
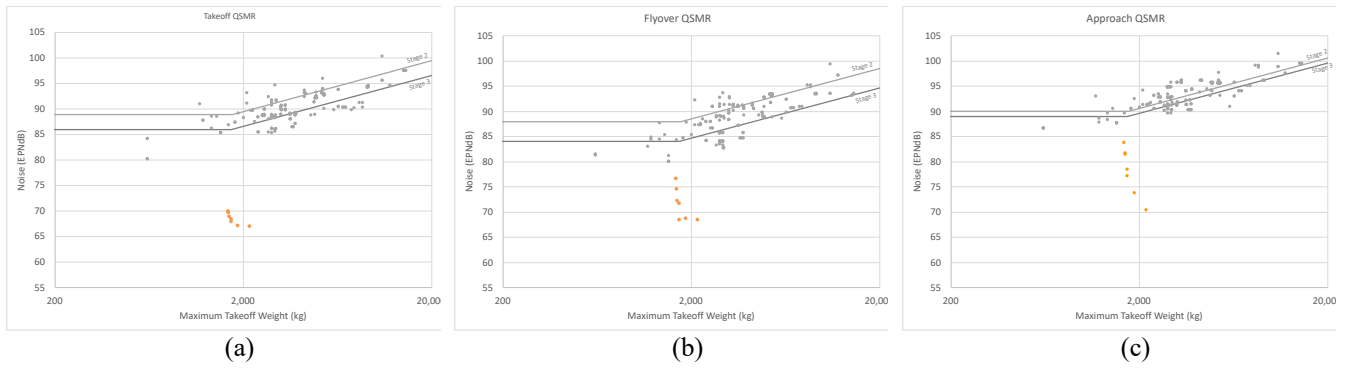
17

Figure 16. QSMR noise and max gross weight with varying tip speed

Table 6. QSMR results with varying tip speed

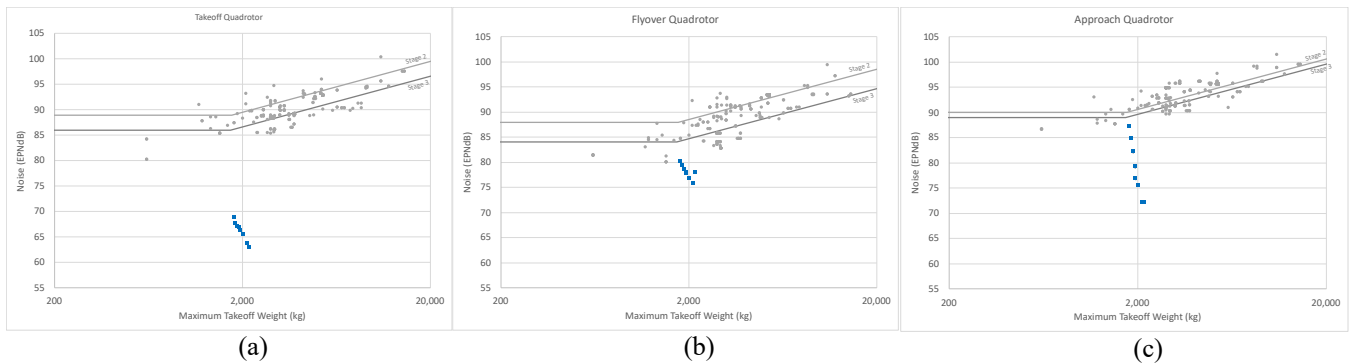| Tip speed (ft/s) | Δ Takeoff (EPNdB) | Δ Flyover (EPNdB) | Δ Approach (EPNdB) | Δ Empty Wt (%) | Δ Block time (%) | Δ Flyaway (%) |
|---|---|---|---|---|---|---|
| 400 | **-1.8** | **-3.9** | **-11.0** | 23% | 9% | 36% |
| 450 | **-1.8** | -3.5 | -7.6 | 11% | **-2%** | 16% |
| 500 | -1.0 | **-3.9** | -4.2 | 4% | -1% | 8% |
| 550 | -0.5 | -0.6 | -2.9 | 3% | -1% | 2% |
| <u>600</u> | | | | | | |
| 650 | 0.8 | 2.3 | 0.3 | -1% | 0% | -4% |
| 700 | 1.1 | 4.3 | 2.4 | **-3%** | 2% | **-5%** |



Figure 17. Quadrotor noise and max gross weight with varying tip speed compared to existing helicopters

**Table 7. Quadrotor results for varying tip speed**

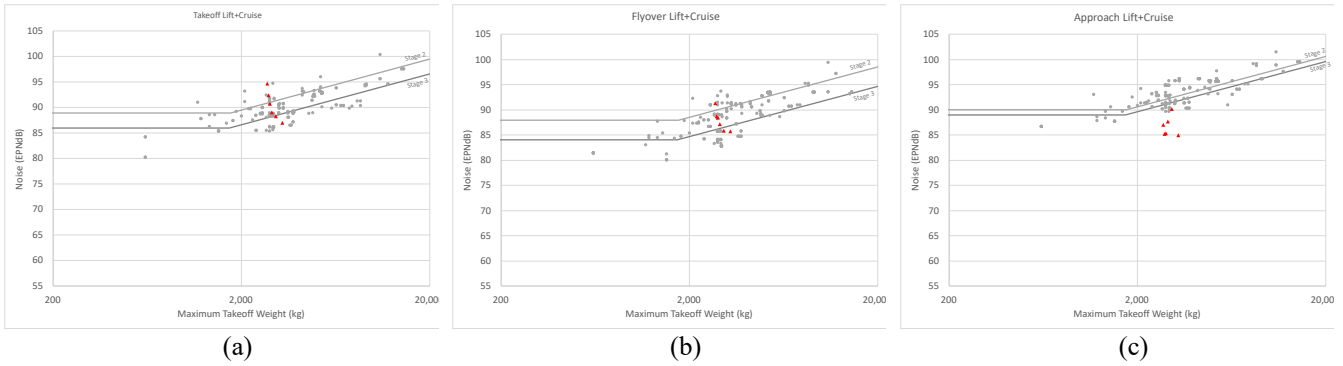| Tip speed (ft/s) | Δ Takeoff (EPNdB) | Δ Flyover (EPNdB) | Δ Approach (EPNdB) | Δ Empty Wt (%) | Δ Block time (%) | Δ Flyaway (%) |
|---|---|---|---|---|---|---|
| 375 | **-3.9** | 0.2 | -7.0 | 9% | 18% | 14% |
| 400 | -3.2 | **-2.0** | **-7.1** | 14% | 10% | 25% |
| 450 | -1.3 | -0.9 | -3.7 | 5% | 7% | 10% |
| 500 | -0.5 | 0.2 | -2.4 | 1% | 4% | 4% |
| <u>550</u> | | | | | | |
| 600 | 0.3 | 0.9 | 3.0 | -3% | -2% | -3% |
| 650 | 0.9 | 1.6 | 5.7 | -7% | **-3%** | -6% |
| 700 | 2.1 | 2.5 | 8.1 | **-9%** | -1% | **-9%** |



(a)   (b)   (c)

**Figure 18. Lift+Cruise noise and max gross weight with varying tip speed**

**Table 8. Lift+Cruise results for varying tip speed**

| Tip speed (ft/s) | Δ Takeoff (EPNdB) | Δ Flyover (EPNdB) | Δ Approach (EPNdB) | Δ Empty Wt (%) | Δ Block time (%) | Δ Flyaway (%) |
|---|---|---|---|---|---|---|
| 350 | **-5.3** | **-2.9** | **-0.3** | 22% | **0%** | 24% |
| 400 | -4.1 | **-2.9** | 5.0 | 12% | **0%** | 12% |
| 450 | -3.3 | -1.5 | 2.4 | 5% | 1% | 5% |
| 500 | -1.7 | -0.3 | 0.1 | 2% | **0%** | 2% |
| <u>550</u> | | | | | 0% | |
| 600 | 2.4 | 2.6 | 1.8 | **-2%** | **0%** | **-2%** |

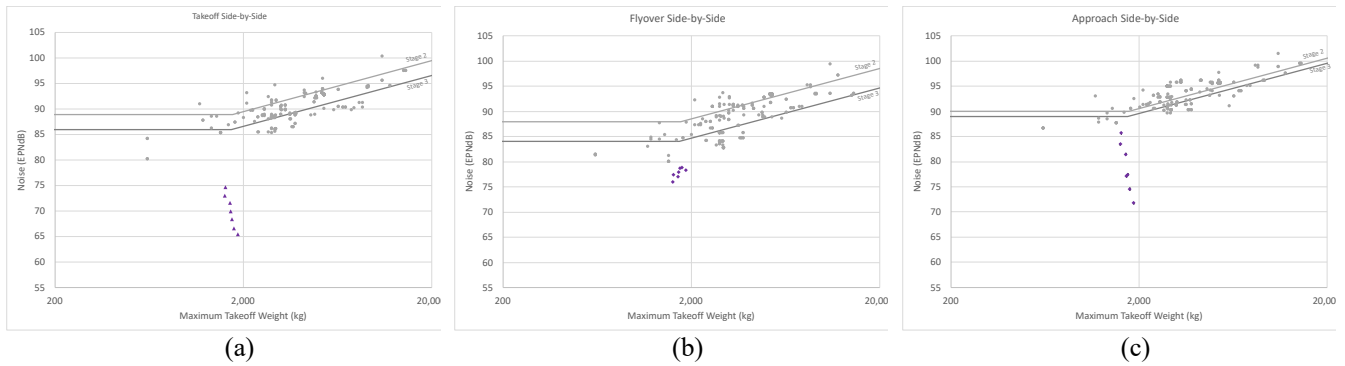(a)              (b)              (c)

**Figure 19. Side-by-Side noise and max gross weight with varying tip speed compared to existing helicopters**

**Table 9. Side-by-Side results for varying tip speed**

| Tip speed (ft/s) | Δ Takeoff (EPNdB) | Δ Flyover (EPNdB) | Δ Approach (EPNdB) | Δ Empty Wt (%) | Δ Block time (%) | Δ Flyaway (%) |
|---|---|---|---|---|---|---|
| 400 | **-4.4** | 0.3 | **-5.4** | 17% | 23% | 9% |
| 450 | -3.2 | 0.9 | -2.6 | 9% | 12% | 4% |
| 500 | -1.5 | 0.7 | 0.3 | 3% | 5% | 1% |
| <u>550</u> | | | | | | |
| 600 | 1.8 | -1.0 | 4.3 | -3% | **-4%** | -1% |
| 650 | 3.2 | **-2.0** | 6.3 | **-8%** | **-4%** | **-6%** |
| 700 | 4.8 | -0.5 | 8.5 | **-8%** | **-4%** | -5% |



| Basic rotor 550 ft/s | Droop at 0.94R 20 degrees | IBC 2/rev 1 degree |
|---|---|---|
| 78.0 EPNdB | 76.3 EPNdB | 76.8 EPNdB |
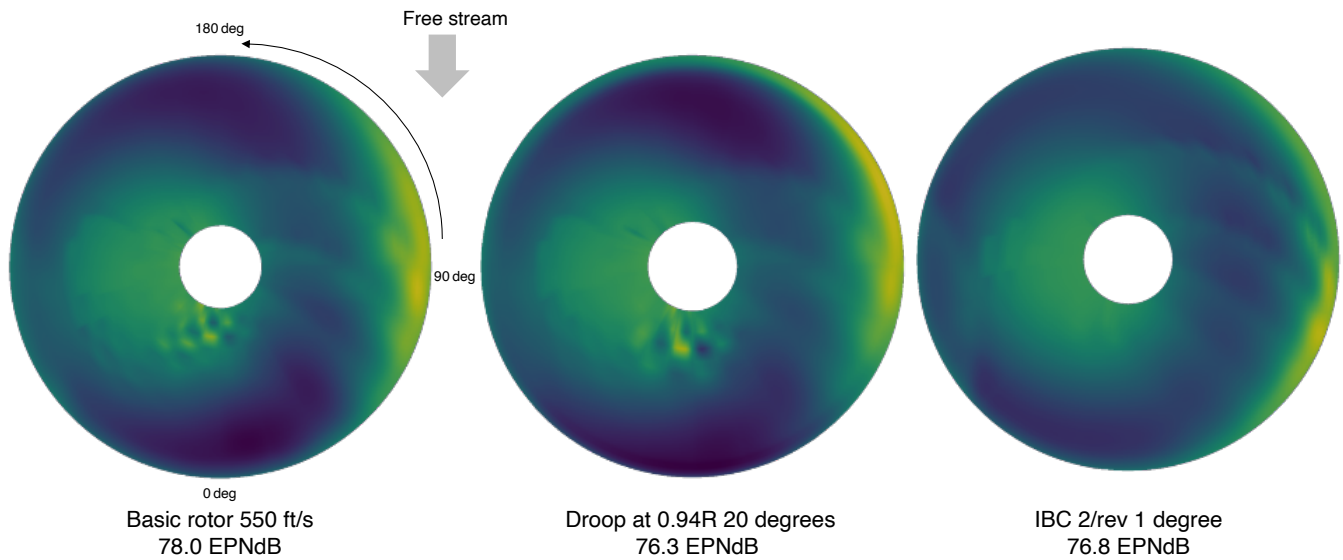
**Figure 20. Side-by-Side rotor 1 (right side) Z-direction loading for Flyover**

Free stream

700 ft/s
85.7 EPNdB

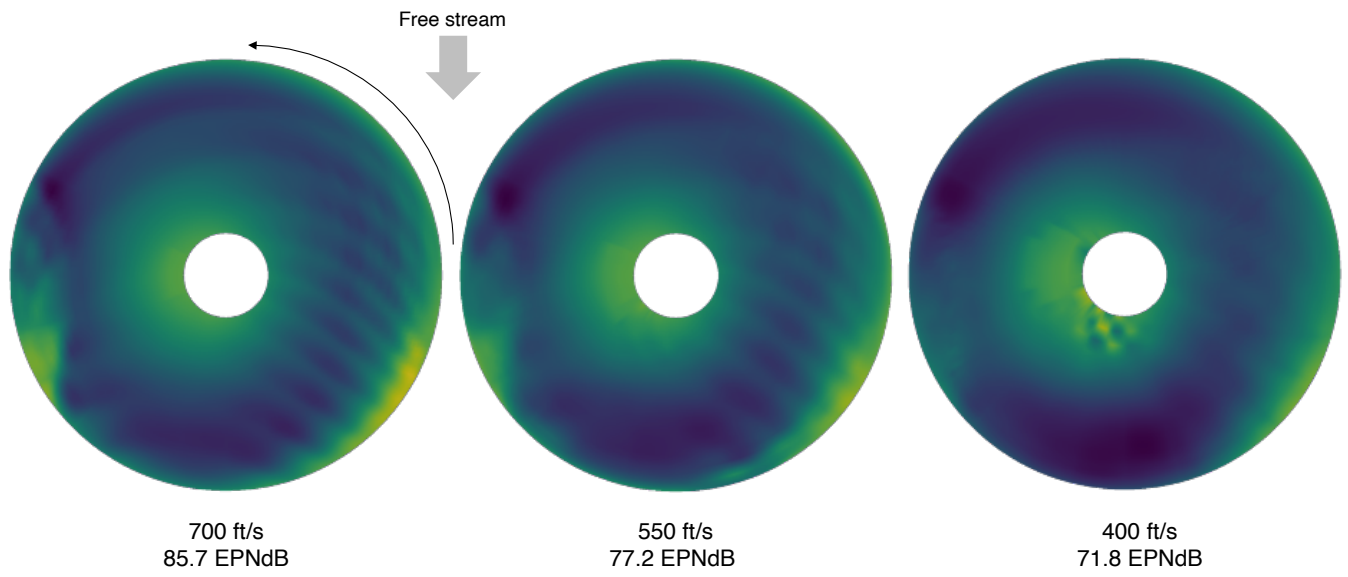550 ft/s
77.2 EPNdB

400 ft/s
71.8 EPNdB

**Figure 21. Side-by-Side rotor 1 (right side) Z-direction loading for Approach**